

# Allan Hills (ALH) 76005, 77302, 78040, 78132, 78158, 78165, 79017, 80102, 81006, 81007, 81008, 81009, 81010, 81012

Polymict Eucrite

1425, 235.5, 211.7, 656, 15.1, 20.9, 310, 471.2, 254.9, 163.5,  
43.8, 229.0, 219.1, 36.7 grams (Total = 4292.4 g)

*Antarctic Finds*

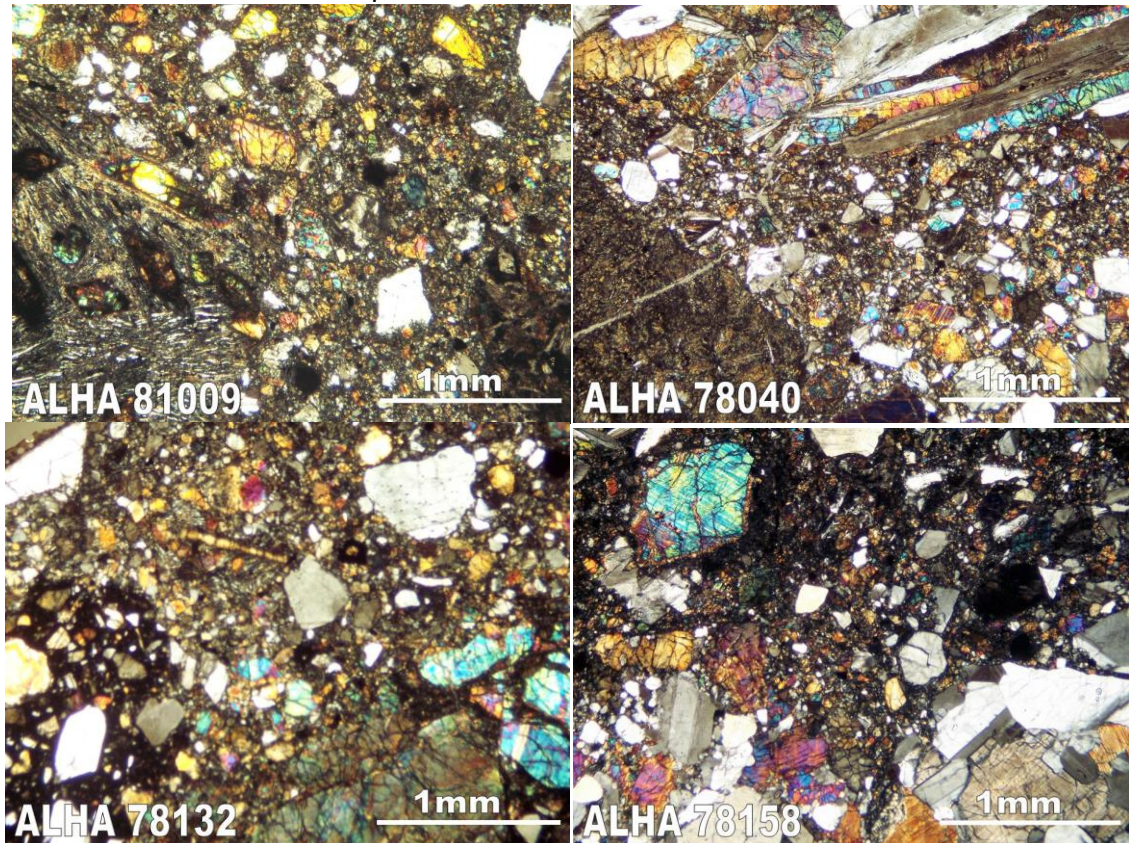


Figure 1: Field photos for several specimens for this pairing group of polymict eucrites: ALH 76005 (top left), ALH A78132 (top right), ALH A81010 (bottom left) and ALH A81006 (bottom right).

## Introduction:

Allan Hills 76005 (or 765) was collected by the joint US-Japan field search for meteorites in 1976-77 (Figure 1). It was described in detail by Olsen, et al. (1978) as

*“pale gray in color and consists of finely divided macrocrystalline pyroxene-rich matrix that contains abundant clastic fragments: (1) Clasts of white, plagioclase-rich rocks. (2) Medium-gray, partly devitrified, cryptocrystalline. (3) Monomineralic fragments and grains of pyroxene, plagioclases, oxide minerals, sulfides, and metal. In overall appearance it is very similar to some lunar breccias.”* Subsequent studies have found a great diversity of basaltic clast textures and compositions, and therefore it is best classified as a polymict eucrite. Samples from the 1976-77, 77-78, and 78-79 field seasons (76, 77, and 78 prefixes) were split between US and Japan (NIPR). The US specimens are currently at NASA-JSC, Smithsonian Institution, or the Field Museum in Chicago. After this initial finding of ALH 76005, the next year’s team recovered one additional mass ALH A77302, and then the third season four additional masses – ALH A78040 and ALH A78132, A78158 and A78165. The joint US-Japan collection effort ended after three years and the US began collecting in the Trans-Antarctic Mountains with the 1979-80 and subsequent field seasons. ALH



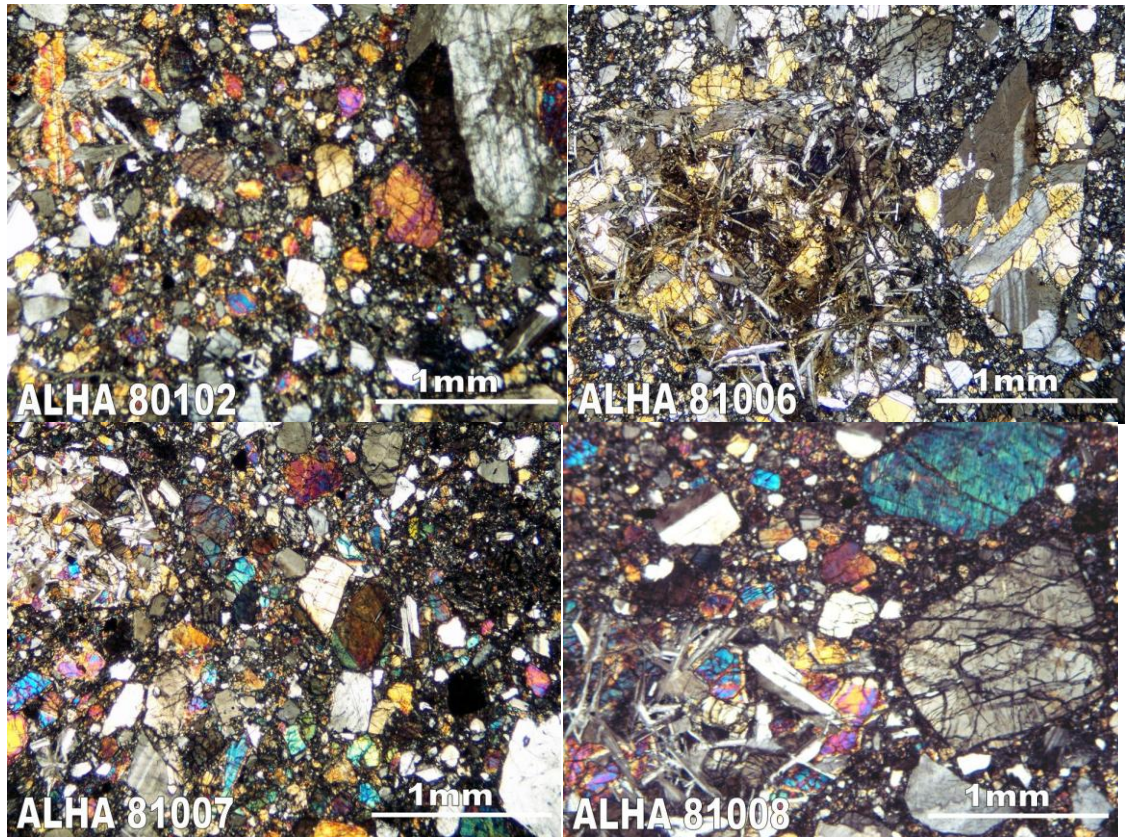


Figure 2: Cross nicols views of eight different samples from the ALH polymict eucrites pairing group. Clasts of various basaltic clasts as well as a small amount of diogenite material can be seen in different views, as well as fragments in the matrix.

A79017 and ALH A80102 were recovered in these first two years, and then in 1981-82 field season 6 additional masses were recovered from the Allan Hills. Of course it took some time to establish pairing of all of these specimens (see Delaney et al., 1984 for a nice summary), but altogether the samples comprise 4292.4 g of material.

### General Petrography:

The ALH polymict eucrites contain a wide range of basaltic clast types (spherulitic, variolitic, coarse- and fine-grained, and subophitic basalts), as well as dark fine-grained material, and some mineral fragments such as metal, oxides, feldspar, and pyroxene. All of these clast types and mineral fragments can be seen in the eight petrographic microscope images (cross-polars) in **Figure 2**. The matrix contains many mineral fragments as well, and careful petrographic studies of the bulk meteorite and clasts were carried out by Fuhrman and Papike (1981); Simon and Papike (1983); Grossman et al. (1981); Olsen et al. (1978); Olsen et al. (1980); Delaney et al. (1984) (for ALH 76005), Simon and Papike (1983); Labotka and Papike (1980); (for ALH 77302), Metzler et al. (1995) (for ALH 78132), Reid and Score (1981) (for ALH 79017), and Treiman and Drake (1985); (for ALH 80102).

The unique modal mineralogy of the ALH pairing group (**Table 1a,b,c**), compared to other polymict eucrites groups such as the Yamato and Elephant Moraine

groups is evident in **Figure 3**, where the ALH group forms a distinct field with respect to plagioclase, and low and high Ca pyroxenes.

Many of these samples were included in consortia organized by A. Reid and a list of clast types was developed for use by the consortia. These are given in **Table 2**, and where later work was carried out after the consortia, we have assigned clast types to the clasts based on information given in the papers.

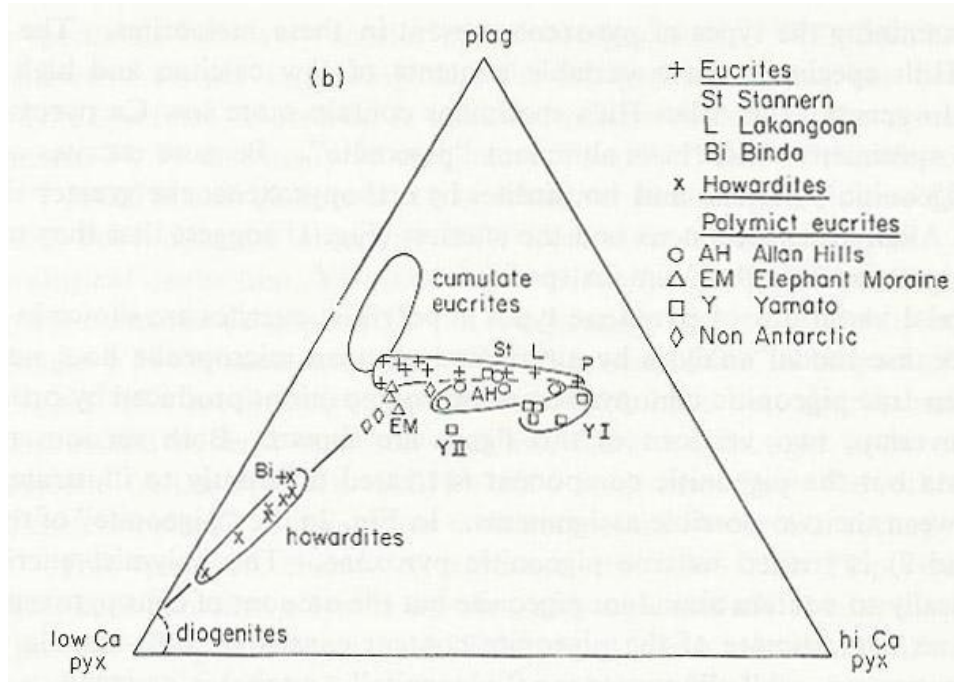


Figure 3: Mineralogic variation in the ALH polymict eucrites (open circles) compared to other polymict eucrites, howardites, and a few select eucrites (from Delaney et al., 1984).

### Mineral Chemistry:

Pyroxene compositions and textures are variable, and have been summarized into four distinct groups by Miyamoto et al. (1979). Group A (Pasamonte type) are characterized by large homogeneous cores with a thin rim of more FeO-rich pyroxene; group B pyroxenes have Fe-Mg zoning from core to rim, but also have exsolution lamellae; group C has pyroxene grains that have two portions that are comprised of group A (zoning and no exsolution) and group B (zoning and exsolution); and group D (Juvinas type) have fine exsolution lamellae with uniform chemical composition. Typical compositions for these four types of pyroxenes are shown in **Figure 4** and the diversity of pyroxene compositions within one paired mass is illustrated in **Figure 5**. Detailed analyses of the pyroxenes from individual specimens are reported by Miyamoto et al. (1979), Fuhrman and Papike (1981), and Simon and Papike (1983) for ALH 76005; Simon and Papike (1981) and Labotka and Papike (1980) for ALH 77302; Metzler et al. (1995) for ALH 78132, and Treiman and Drake (1985) and Metzler et al. (1995) for ALH 80102.

All pyroxenes analyzed in ALH 76005 have negative Eu anomalies, and feldspars have positive Eu anomalies (**Figure 6**; Nakamura and Masuda, 1980). Furthermore, the range of bulk REE abundances is large amount the different kinds of pyroxene (**Figure 6**).

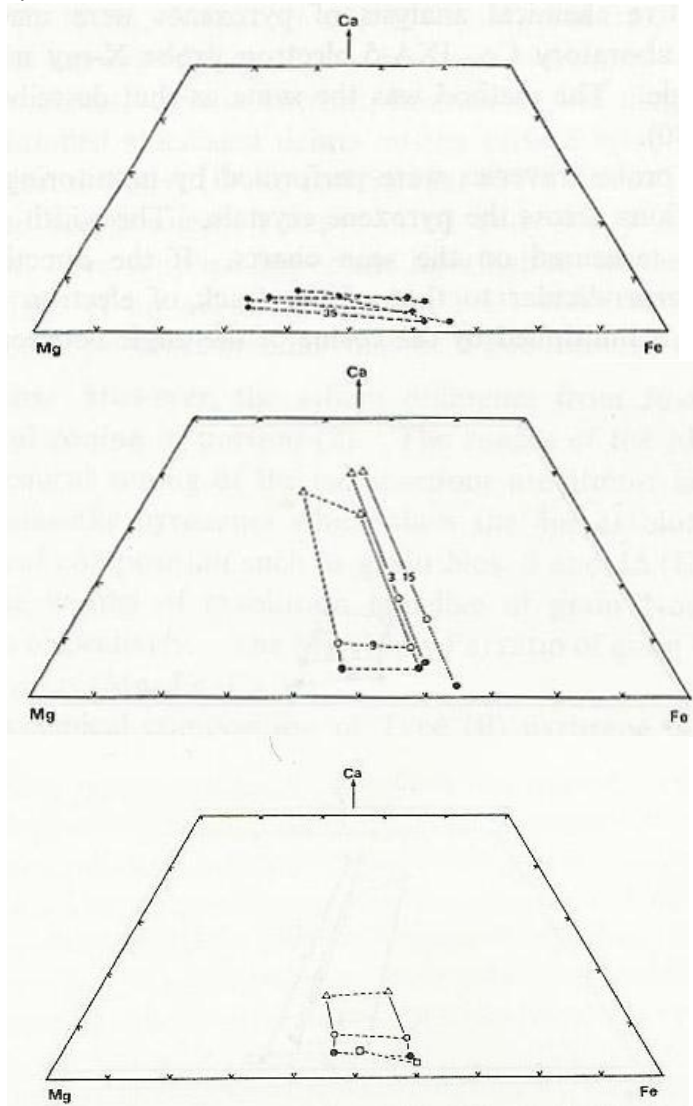


Figure 4: Pyroxene quadrilateral diagrams for pyroxenes from several clasts in ALH 76005, illustrating the several different kinds of clast types in the ALH polymict eucrites pairing group (from Miyamoto et al., 1979).

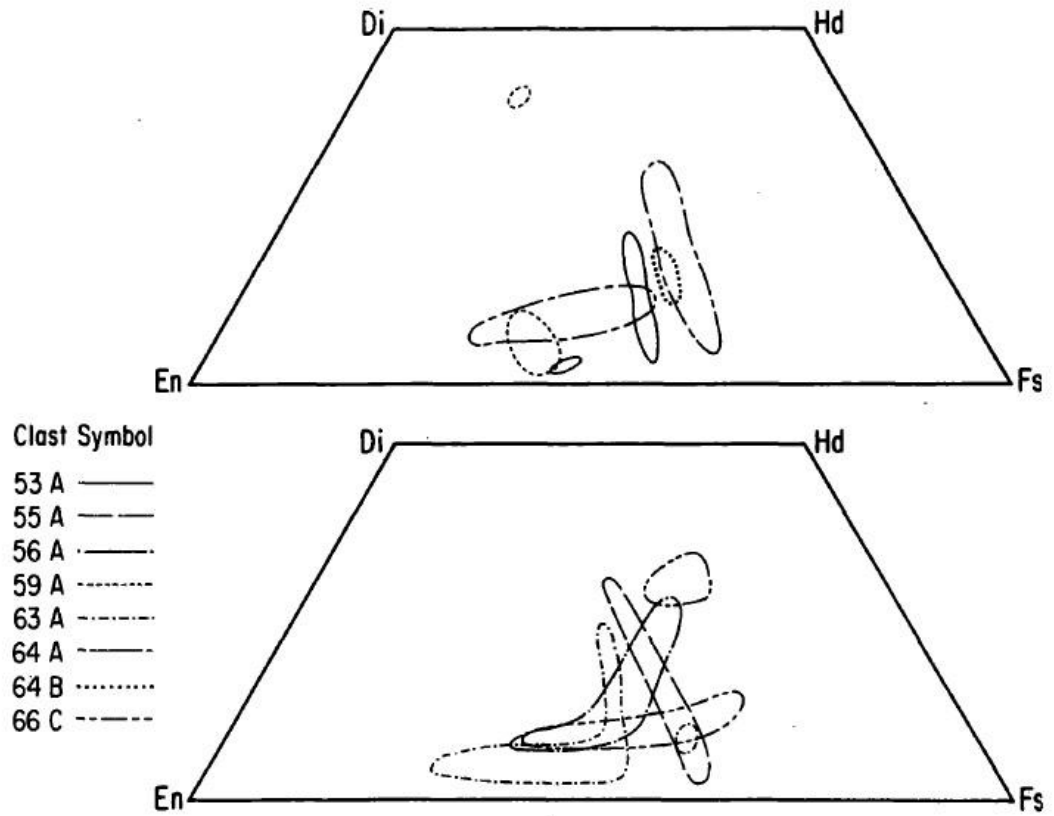


Figure 5: Pyroxene quadrilateral diagrams for pyroxenes from several clasts in ALH 80102, illustrating the several different kinds of clast types in the ALH polymict eucrites pairing group (from Treiman and Drake, 1985).

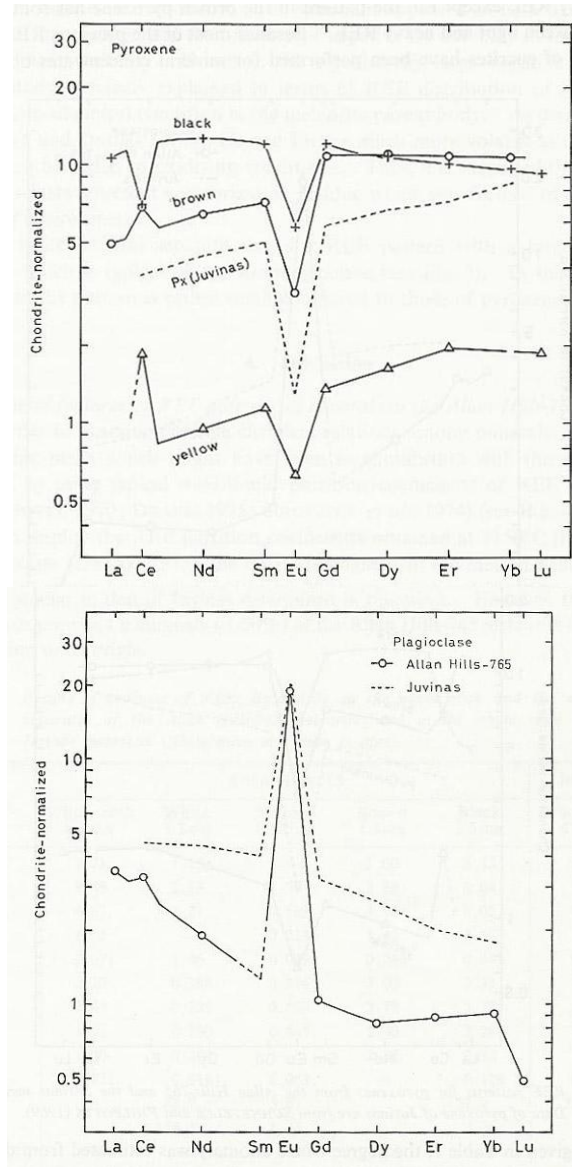


Figure 6: Rare earth element diagrams for pyroxenes and plagioclase from the ALH 76005 polymict eucrites, illustrating the variation in pyroxene compositions, as well as the large Eu anomaly in the plagioclase (from Nakamura and Masuda, 1980).

#### Whole-Rock and Clast Chemistry:

The bulk rock composition of samples from the ALH-pairing group falls in the middle of the region defined by polymict eucrites, in terms of major ( $MgO$  and  $Al_2O_3$ ) and trace (Sc, Sm) elements (**Figure 7; Table 3 and 4**). Clasts and whole rock chemistry of the various pairing masses were studied by the following: ALH 76005: Smith and Schmitt (1981), Nakamura and Masuda (1980), Metzler et al. (1995), Mittlefehldt (1979), Wooden et al. (1981); ALH A77302: Hertogen et al. (1981); Smith and Schmitt (1981), Fukuoka and Nakamura (1981), Wooden (1981), Delaney et al. (1984); ALH A78040: Smith and Schmitt (1981), Wooden et al. (1981), Delaney et al. (1984); ALH A78132: Smith and Schmitt (1981), Metzler et al. (1995), Wooden et al. (1981), Warren et al. (2009); ALH A78158: Smith and Schmitt (1981), Wooden et al. (1981);

ALH A78165: Smith and Schmitt (1981), Wooden et al. (1981); ALH 80102: Metzler et al. (1995); ALH 81007: Mittlefehldt and Lindstrom (2003); ALH 81009: Mittlefehldt and Lindstrom (2003). Additional partial analyses of samples (whole rock and clasts) are presented in Fukuoka and Nakamura (1981) and Nakamura and Masuda (1980).

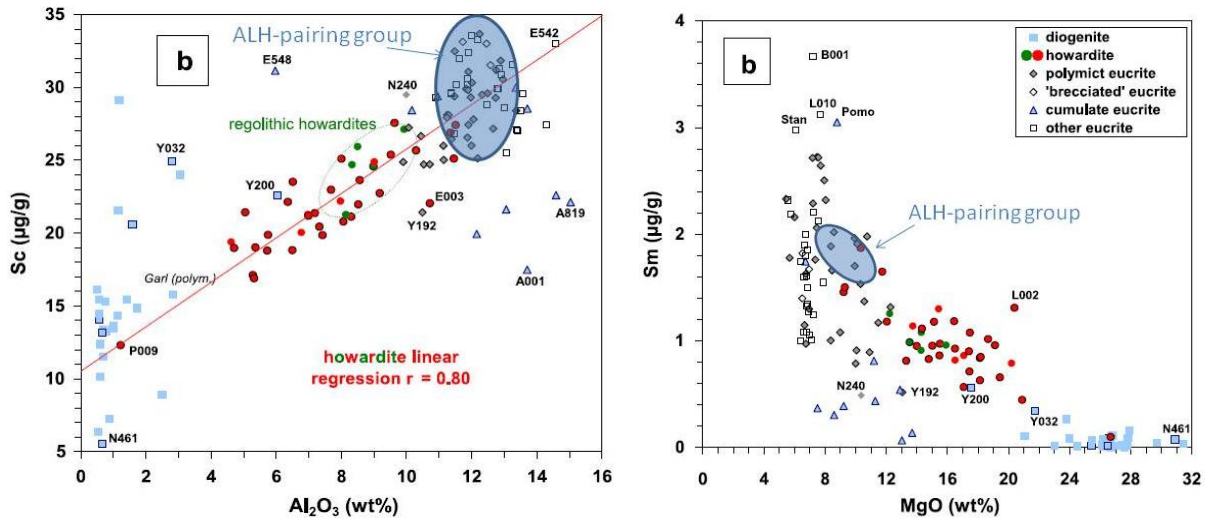


Figure 7: Bulk rock analyses of ALH pairing group samples (in blue ellipse) compared to H-E-D meteorite analyses of Warren et al. (2009).

Table 1 a: modal analyses of Allan Hills polymict eucrites whole rock (from Delaney et al., 1984).

sample	1	2	3	4	5	6	7	8	9	10	11
generic	76005	77302	78040	78158	78165	81006	81007	81008	81009	81010	81012
Split											
Oliv	nd	nd	tr	nd	Nd	nd	0.4	nd	nd	nd	nd
Opx	15.1	14.9	9.0	7.7	7.7	13.5	18.7	20.4	12.7	10.7	9.3
Pig	25.4	29.7	31.6	21.2	29.1	30.8	37.3	32.2	32.2	30.4	29.6
Aug	11.9	10.1	11.5	15.9	16.2	13.6	5.7	9.9	13.0	12.2	14.0
Feld	42.9	39.9	42.6	45.9	43.5	35.4	35.4	34.1	38.4	41.0	41.2
Sil	4.3	4.2	4.2	2.3	3.0	5.5	1.7	2.4	3.0	5.0	4.7
Ilm	0.1	0.6	0.6	0.4	1.0	0.5	0.2	0.5	0.8	0.4	0.9
Cm	0.3	0.1	0.1	0.1	0.3	0.2	0.4	0.2	tr	0.1	0.2
Phos	nd	0.2	0.2	nd	0.1	0.1	0.1	0.1	tr	0.2	0.1
Troil	nd	tr	0.3	nd	nd	0.4	0.1	nd	tr	0.1	tr
Metal	nd	tr	0.1	0.3	nd						
gyps	nd	nd	nd	nd	nd	nd	0.1	nd	tr	tr	nd
Area	22	132	357	24	38	78	96	75	41	175	101
# pts	788	1175	2769	953	925	940	949	968	870	952	970

**Table 1 b: modal analyses of Allan Hills polymict eucrites whole rock**

sample	76005	77302,34
reference	FP80	LP80
comments		
matrix	28.5	-
Mineral clasts	61.3	93.9
	33.5	54.2
	27.2	35.7
Lithic clasts	8.2	4
Fused soil	2.0	3.5
<b>Total</b>		

FP80 = Fuhrman and Papike (1980); LP80 = Labotka and Papike (1980)

**Table 1 c: modal analyses of Allan Hills polymict eucrites clasts (Simon and Papike, 1983)**

sample	1	2	3	4	5	6
	76005	76005	76005	76005	77302	77302
comments	,17	,10	,20	,41	,58	,74
type	C		B	E	B	E
“Pyroxene”	63.6	43.4	48.3	67.5	65.1	53.4
Feldspar	35.6	36.8	38.4	32.0	30.9	42.8
Silica	-	-	0.1	0.4	-	1.4
Ilmenite	0.8	2.5	1.3	0.1	-	0.4
Troilite	-	0.4	2.5	-	4.0	tr
Metal	-	-	tr	-	tr	-
Gypsum						
mesostasis	-	16.9	9.4	-	-	2.0

**Table 2: Clast types used in Reid Consortia**

Type	description
A	White, chalky, feldspar-rich
B	Dark, fine grained
C	Coarser grained, pyrox.-feldsp. eucritic
D	Shock melted fragments in fine matrix
E	Eucrites fine grained igneous
F	Pyroxenite
G	Oxide fragments
H	Feldspar and oxide
I	Single crystal grains

**Table 3: Bulk analyses of Allan Hills polymict eucrites**

reference	1	2	2	2	2	2	2	2	2	3	4	5
Weight (mg)	45.7	391.4	235.8	149.0	148.7	144.9	71.4	26.7	114.8			
comments	76005	76005	77302	78040	78132	78132	78158	78158	78165	76005	76005	76005
split		23	53	44	28	39	13-1	13-2	13	broad beam	wet	wet
SiO <sub>2</sub>	48.5(8)									49.29	50.31	48.21
TiO <sub>2</sub>	0.55(12)	0.39	0.54	0.42	0.62	0.67	0.41	0.50	0.71	0.57	0.75	0.78
Al <sub>2</sub> O <sub>3</sub>	12.4(1)	12.1	12.7	12.6	12.0	12.6	12.5	12.4	12.3	13.28	12.57	12.02
Cr <sub>2</sub> O <sub>3</sub>	0.3541(7)	0.31	0.34	0.35	0.38	0.33	0.32	0.32	0.32	0.27	0.40	0.40
FeO	20.07(4)	18.6	17.7	18.8	19.3	18.4	20.0	19.6	20.1	19.62	18.06	18.89
MnO	0.554(4)	0.51	0.52	0.52	0.53	0.51	0.50	0.51	0.53	0.56	0.58	0.52
MgO	7.54(59)	5.7	9.0	7.9	7.8	5.9	5.6	6.8	7.2	6.79	6.93	7.66
CaO	9.47(50)	8.8	8.3	10.1	8.7	9.5	10.3	10.6	9.7	9.20	9.90	9.08
Na <sub>2</sub> O		0.46	0.46	0.45	0.45	0.50	0.42	0.47	0.40	0.49	0.44	0.56
K <sub>2</sub> O	0.0642(64)	0.055	0.037	0.055	0.047	0.056	0.051	0.045	0.048	0.08	0.06	0.06
P <sub>2</sub> O <sub>5</sub>												0.10
Total										100.15	100.00	99.83
Sc ppm	33.64	32	25	30	31	34	25	27	31			
V ppm	68.3	66	73	72	77	66	72	77	81			
Co ppm	6.72	5.2	7.3	7.2	5.9	10.1	4.6	8.0	8.6			
Ni ppm	60	20	10	10	20	40	20	100	130			
Cu ppm												
Zn ppm												
Ga ppm												
Ge ppm												
Sr ppm	82	80	80	100	80	90	80	130	110			
Zr ppm												
Ba ppm	35	35	35	30	36	65	19	17	35			
La ppm	3.87	3.3	2.1	3.5	2.4	3.7	1.3	1.5	2.5			
Ce ppm	8.95											
Nd ppm	9.1	10		8		12						

Sm ppm	2.372	6		7		9			
Eu ppm	0.698	2.10	1.48	2.18	1.85	2.80	0.92	1.13	1.58
Tb ppm	0.632	0.65	0.52	0.67	0.65	0.70	0.62	0.58	0.62
Dy ppm	4.63								
Yb ppm	2.26	0.49	0.36	0.53	0.42	0.60	0.25	0.34	0.41
Lu ppm	0.294	2.1	1.5	2.2	1.8	2.5	1.4	1.4	1.8
Hf ppb	1.44	31	27	29	32	32	31	30	30
Ta ppb	0.187	1500	1200	1500	1900	1600	1400	1400	1400
W ppb	0.58								
Re ppb									
Os ppb									
Ir ppb									
Pt ppb									
Au ppb	8.95	5	-						
Th ppb	0.366	0.31	0.24	0.28	0.30	0.31	0.20	0.20	0.24
U ppb									
Cs ppm		0.36	0.29	0.35	0.27	0.44	0.36	0.44	0.32
Br ppm	0.286								
<i>technique:</i>	<i>INAA</i>								

1 = Grossman et al. (1981); 2 = Smith and Schmitt (1981); 3 = Fuhrman and Papike (1981); 4 = Olsen et al. (1978); 5 = Miyamoto et al. (1979)

**Table 3: Bulk analyses of Allan Hills polymict eucrites (continued)**

reference	3	3	7	7	4	4	4	4	4	4	4
weight	45.04	99.52	337	375							
comments	81007	81009	78132	78132	76005	77302	78040	78132	78132	78158	78165
split	15	27	99	102	16	55	46	24	25	14	14
SiO <sub>2</sub>			50.07	51.00	47.92	48.54	48.52	48.89	49.33	48.65	49.01
TiO <sub>2</sub>			0.62	0.55	1.04	0.61	0.75	0.59	0.87	0.94	0.70
Al <sub>2</sub> O <sub>3</sub>			13.41	11.91	12.56	12.00	13.46	12.57	12.93	11.44	12.81
Cr <sub>2</sub> O <sub>3</sub>	0.283	0.358	0.36	0.43	0.34	0.39	0.37	0.37	0.35	0.41	0.25
FeO	14.3	20.0	16.75	17.89	19.23	18.66	18.31	18.39	17.57	20.01	18.57
MnO			0.47	0.55	0.57	0.60	0.62	0.64	0.59	0.60	0.62
MgO			7.24	9.67	7.16	8.94	7.51	8.70	7.31	8.02	7.11
CaO	9.9	11.4	9.67	8.42	9.87	9.08	9.88	9.06	10.02	9.28	9.89
Na <sub>2</sub> O	0.417	0.460	0.47	0.42	0.43	0.33	0.44	0.35	0.38	0.37	0.38
K <sub>2</sub> O	170				0.09	0.07	0.07	0.06	0.05	0.08	0.09
P <sub>2</sub> O <sub>5</sub>					0.03	0.04	0.06	0.07	0.06	0.02	0.06
Total					99.24	99.26	99.99	99.69	99.46	99.82	99.49
Sc ppm	19.6	31.3	27.6	26.8							
V ppm			64	78							
Co ppm	5.25	16.9	5.3	6.6							
Ni ppm	60	190	14	16							
Cu ppm											
Zn ppm											
Ga ppm			<5	<1.0							
Ge ppm											
Sr ppm	98	87	90	54							
Zr ppm											
Ba ppm	20	34	<80	<80							
La ppm	5.01	3.84	2.71	3.04							
Ce ppm	14.1	9.4									
Nd ppm	10	8									
Sm ppm	2.36	2.42	1.82	1.50							
Eu ppm	0.578	0.665	0.64	0.55							

Tb ppm	0.415	0.580		
Dy ppm				
Yb ppm	1.04	2.22		
Lu ppm	0.144	0.335	0.27	0.24
Hf ppb	0.56	1.73	1.00	1.19
Ta ppb	71	223		
W ppb				
Re ppb				
Os ppb				
Ir ppb		8.9	<3	0.87
Pt ppb				
Au ppb	1.2	3.7		
Th ppb	730	550		
U ppb	142	-		
Cs ppm				
Br ppm				

3 = Mittlefehldt and Lindstrom (2003); 4 = Wooden et al. (1981); 7 = Warren et al. (2009)

**Table 4: Analyses of igneous clasts from Allan Hills polymict eucrites**

reference	3	1	5	5	5	5	5	6	6	6	6	6	4	4	4	4	4
weight	108.65	5.02 mg	20.5 mg	24.8 mg	132.3 mg	38.1 mg	33.9 mg	15.25	538.3	57.9	291.45	36.1					
comments	81009	76005	76005	76005	78132	80102	80102	80102	80102	80102	80102	80102	76005	76005	77302	78040	78132
Clast type			C	C	C	C	C	Mesost.	C	C	C	C	C	B	dark	C	E
split	40		69 1a1	69 1a2	92	28	94	44	28	30	31	33	17	20	27	24	30
SiO <sub>2</sub>													52.15	49.65	51.50	48.34	49.65
TiO <sub>2</sub>		0.66	0.72	-	0.63	0.57	0.72						0.90	0.91	1.01	0.65	0.93
Al <sub>2</sub> O <sub>3</sub>		13.9	8.04	12.11	12.91	14.63	15.66						13.87	12.47	12.52	17.12	12.52
Cr <sub>2</sub> O <sub>3</sub>	0.322	0.3544	0.222	0.269	0.264	0.202	0.188						0.30	0.31	0.39	0.30	0.41
FeO	19.5	17.83	24.21	17.30	17.52	11.84	13.78						12.93	18.01	15.01	13.94	17.15
MnO		0.401	0.738	0.501	0.495	0.316	0.402						0.68	0.54	0.48	0.35	0.51
MgO		7.50	9.59	7.00	7.84	5.74	5.57						7.16	6.02	7.22	6.57	7.29
CaO	11.9	10.8	9.12	9.40	8.86	10.14	11.60						10.76	10.29	10.18	11.11	9.94
Na <sub>2</sub> O	0.403	0.668	0.287	0.426	0.509	0.577	0.695						0.61	0.62	0.61	0.57	0.58
K <sub>2</sub> O	170	0.0504	0.017	0.035	0.049	0.043	0.0503						0.05	0.11	0.08	0.10	0.07
P <sub>2</sub> O <sub>5</sub>													0.20	0.10	0.06	0.09	0.12
Total													99.61	99.03	99.06	99.14	99.17
Sc ppm	31.3	38.31	41.8	27.5	28.3	28.7	24.4	34.41	32.06	32.33	32.11	13.38					
V ppm		71.6	75.0		71	59.2	40.3										
Co ppm	3.35	17.26	6.6	11.1	5.92	6.77	6.00	95.1	9.08	7.94	8.50	4.45					
Ni ppm		<440	<60	<40	<20	<30	13	280	25	<28	18	<30					
Cu ppm																	
Zn ppm			42	<20	27	<35	<25										
Ga ppm			<1.2	1.8	2.2	1.8	3.0	2.1	1.3	<2.6	<3.3	1.6					
Ge ppm																	
Sr ppm	103	75	91	<60	84	98	<90	<260	80	115	95	100					
Zr ppm	60		<50	<60	44	50	50										

Ba ppm	34	<60	<30	36	29.9	30	36	<470	42	<125	81	<163
La ppm	3.52	1.24	4.49	3.14	0.74	2.00	2.91	5.95	2.24	2.62	5.63	2.87
Ce ppm	9.1	3.24	9.25	7.70	6.00	7.87	7.13	17.3	7.54	7.23	15.53	3.1
Nd ppm	6	<5.1	8.60	6.32	1.60	4.43	5.60	12.3	5.06	3.7	12.0	4.7
Sm ppm	2.24	0.898	2.83	2.12	0.54	1.35	1.92	3.7	1.65	1.69	3.5	1.35
Eu ppm	0.679	0.457	0.43	0.60	0.51	0.63	1.04	0.762	0.729	0.689	0.885	0.601
Tb ppm	0.499	0.236	0.69	0.48	0.16	0.33	0.46	0.794	0.384	0.39	0.786	0.28
Dy ppm		2.21	4.74	3.02	1.75	2.05	2.95					
Ho ppm								1.23	0.56	0.62	1.08	0.34
Yb ppm	2.12	1.11	3.00	1.85	1.09	1.26	1.83	3.09	1.60	1.77	2.81	0.71
Lu ppm	0.319	0.192	0.45	0.28	0.18	0.19	0.27	0.48	0.247	0.276	0.408	0.11
Hf ppb	1.63	0.786	1.63	1.13	1.24	1.51	1.20	3.05	2.14	1.89	3.62	0.27
Ta ppb	197	106	0.19	0.16	0.15	0.21	0.13	0.64	0.28	0.28	0.51	0.28
W ppb		<530	250	<200	<150	<150	<400	350	<110	<170	<130	<130
Re ppb												
Os ppb												
Ir ppb												
Pt ppb												
Au ppm		2.5						<0.2	<0.2	<0.7	0.3	<2
Th ppb	510	127	240	250	270	400	450	800	530	450	1060	<170
U ppb			88	69	66	130	120	<1200	130	<200	210	<200
Cs ppm												
Br ppm		<0.18										
Se ppb		490			<900							

3 = Mittlefehldt and Lindstrom (2003); 1 = Grossman et al. (1981); 5 = Metzler et al. (1995); 6 = Treiman and Drake (1985); 4 = Wooden et al. (1981)

## Radiogenic Isotopes

Age dating of the ALH polymict eucrites has consisted of Ar-Ar, Rb-Sr, Sm-Nd, and Lu-Hf studies. Ar-Ar dating of ALH 76005 by Kaneoka et al. (1981), ALH 77302 by Spangler et al. (1985) and ALH 76005, ALH 78132, and ALH 80102 by Kunz et al. (1995) have all yielded ages between 3.0 and 4.0 Ga, indicating some disturbances to the Ar system (**Figures 8 and 9**).

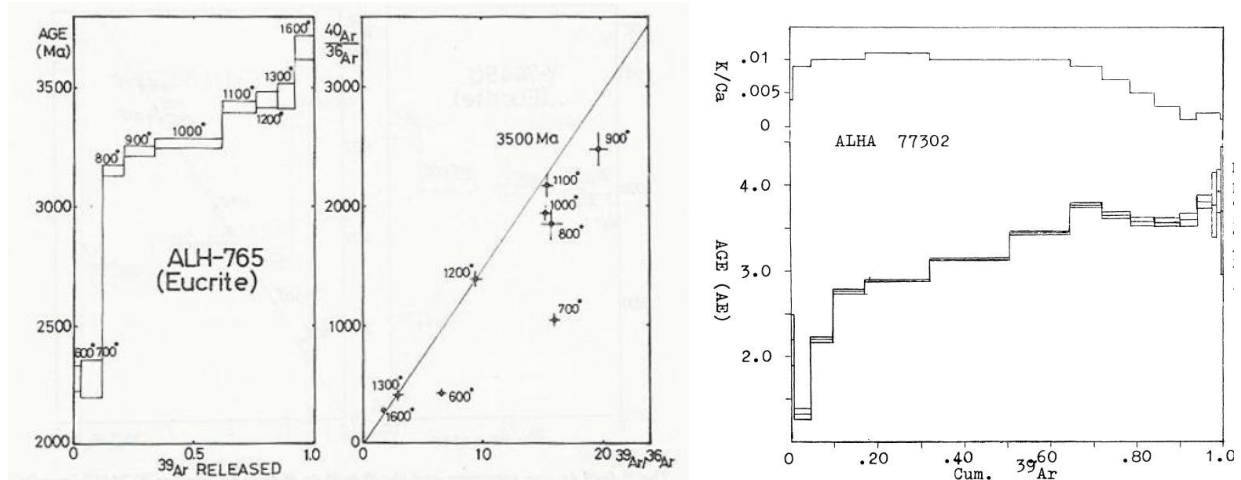


Figure 8: Ar release and age information for ALH 76005 (from Kaneoka, 1981) and ALH 77302 (from Spangler et al., 1985). Both yield ages between 3.0 and 3.5 Ga.

Dating with the Rb-Sr system was done by Wooden et al. (1983) and yields an age of 4.63 (+/- 0.19) Ga by using a number of paired ALH and Yamato polymict eucrites (**Figure 10**). Application of the Sm-Nd system yields similar ages by Nakamura et al. (1983) for ALH 76005 and for several polymict eucrites by Wooden et al. (1983) - 4.52 and 4.56 Ga, respectively (**Figure 11**). And finally, the Lu-Hf system was used to help define the decay constant for this system, yielding a value of  $1.962 \times 10^{-11} \text{ yr}^{-1}$  (Patchett and Tatsumoto, 1980) (**Figure 12**)

## Cosmogenic Isotopes

Evans et al. (1979) noted that ALH 76005 must have a short terrestrial residence time based on its  $^{26}\text{Al}$  content. And  $^{14}\text{C}$  measurements indicated that the residence time must be  $> 34 \text{ Ka}$  (Fireman, 1979). Later measurements by Herpers verified this with terrestrial ages (based on  $^{10}\text{Be}$ ,  $^{53}\text{Mn}$ ,  $^{26}\text{Al}$ ) of  $120 \pm 50 \text{ Ka}$ .

Cosmic ray exposure ages were determined by several groups and using different isotopes. Herpers et al. (1995) measured ALH 76005, 78132, 79017, 80102, 81008, 81009, and 81010, and found ages of 7.3 to 8.3 Ma based on  $^{53}\text{Mn}/^{21}\text{Ne}$ , and ages of 7.7 to 8.8 Ma based on  $^{21}\text{Ne}$ . Later, Welten et al.

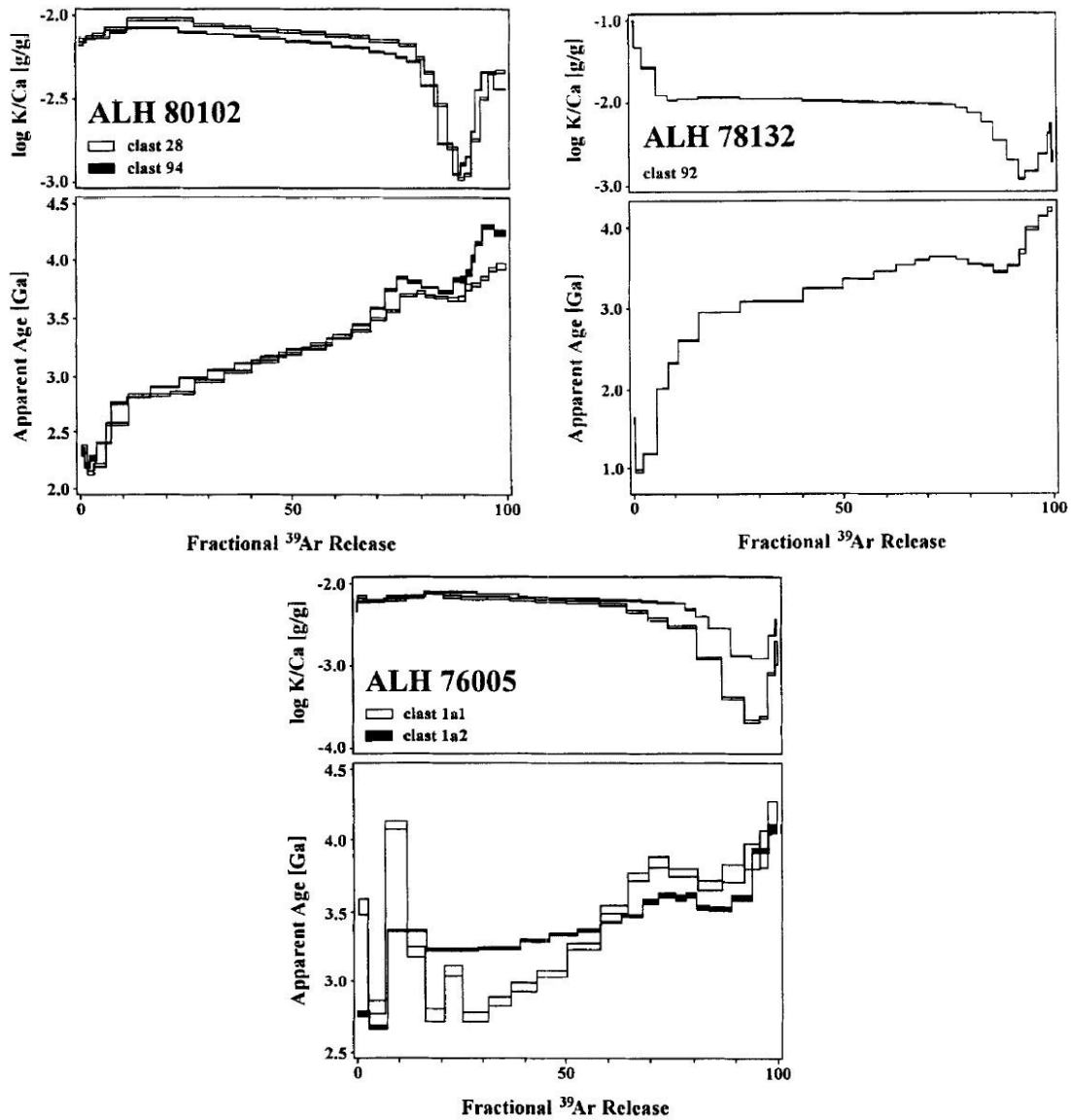


Figure 9: Ar release and age information for ALH 76005, ALH 78132, and ALH 80102 (from Kunz et al., 1995). All yield disturbed ages between 3.0 and 4.0 Ga.

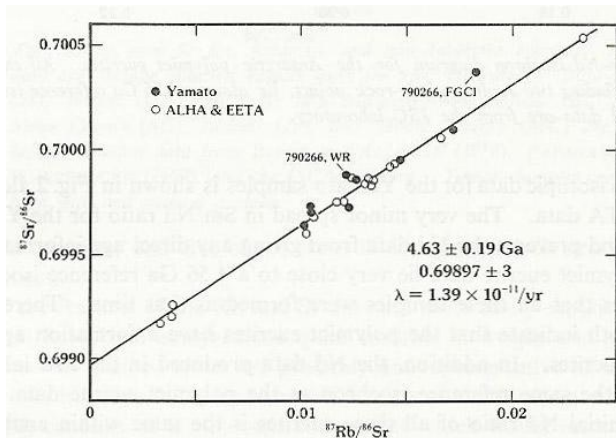


Figure 10: Rb-Sr isotopic diagram for ALH 76, 77, and 78 meteorites from Wooden et al. (1981) showing an isochron of 4.63 Ga.

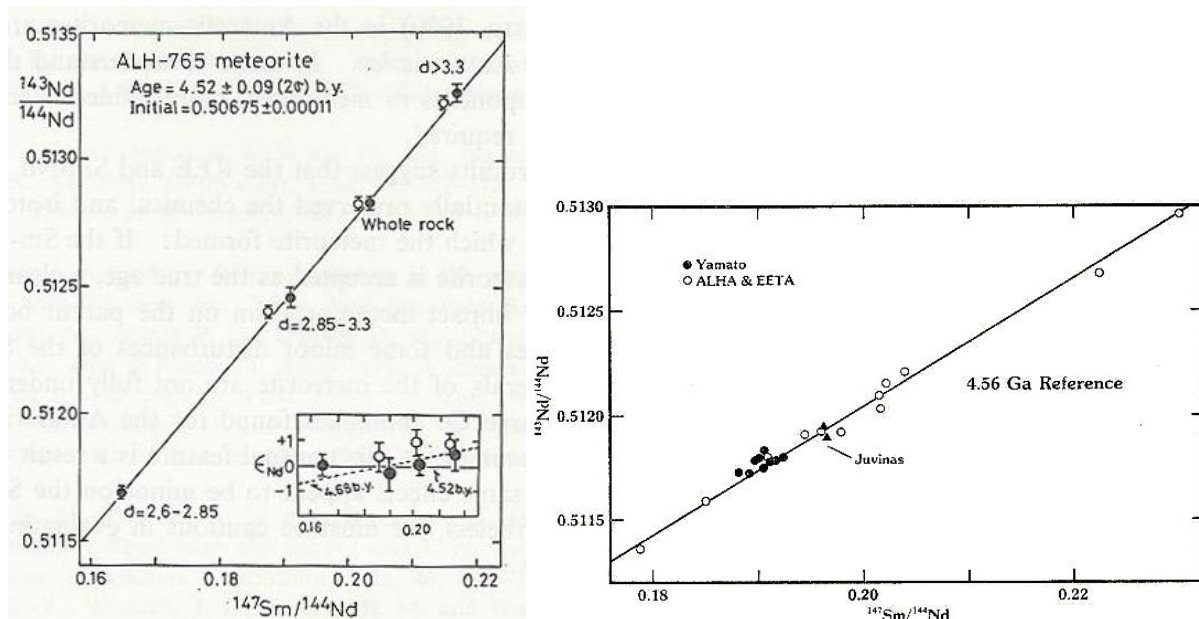


Figure 11: Sm-Nd age for ALH 76005 from Nakamura et al. (1983) and ALH meteorites (76, 77, 78) from Wooden et al. (1981) both indicating an old age for the ALH pairing group (4.52 and 4.56 Ga, respectively).

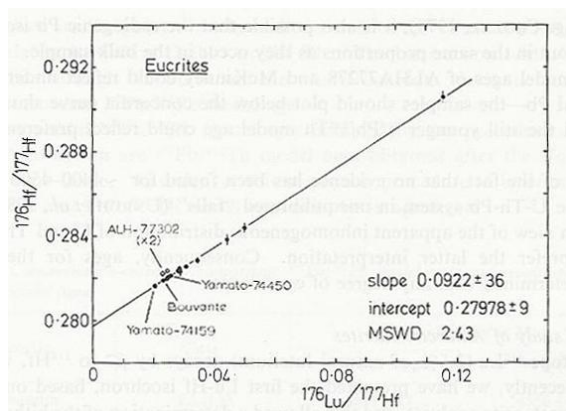


Figure 12: First Lu-Hf isochron for the eucrites (from Tatsumoto and Patchett, 1980) showing an ancient age; note that ALH 77302 samples are not included in the age regression.

(1997) report ages of 10.3(2.1) Ma and 13.1(1.3) Ma based on  $^{21}\text{Ne}$  and  $^{38}\text{Ar}$ , respectively, for ALH 78132 (see also Eugster and Michel, 1995).

### Other Isotopes

ALH 76005 was first measured for oxygen isotopes by Clayton et al. (1979), and found to be close to and on the line defined by other HED's. A clast from their sample was also analyzed and found to be slightly offset from the HED line. There has been no additional work on that clast, but additional analyses by Wiechert et al. (2004) on ALH 76005 and ALH 78132 show overlap with the line defined by

HED, albeit with a little scatter that could be attributed to the polymict nature of the ALH samples (Figure 13).

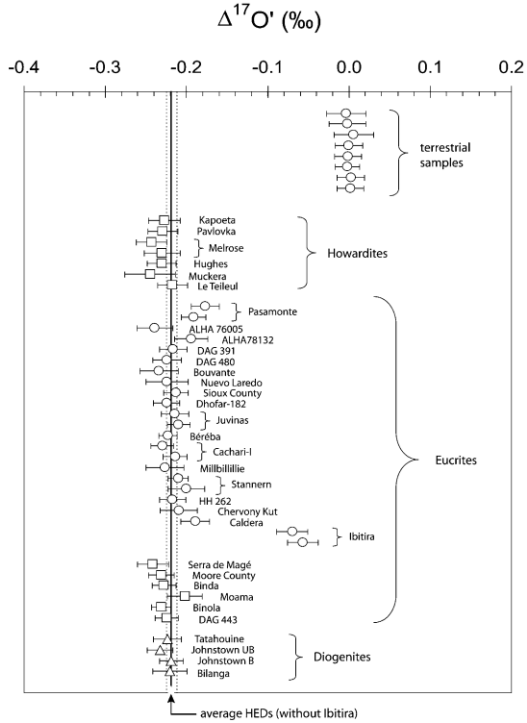
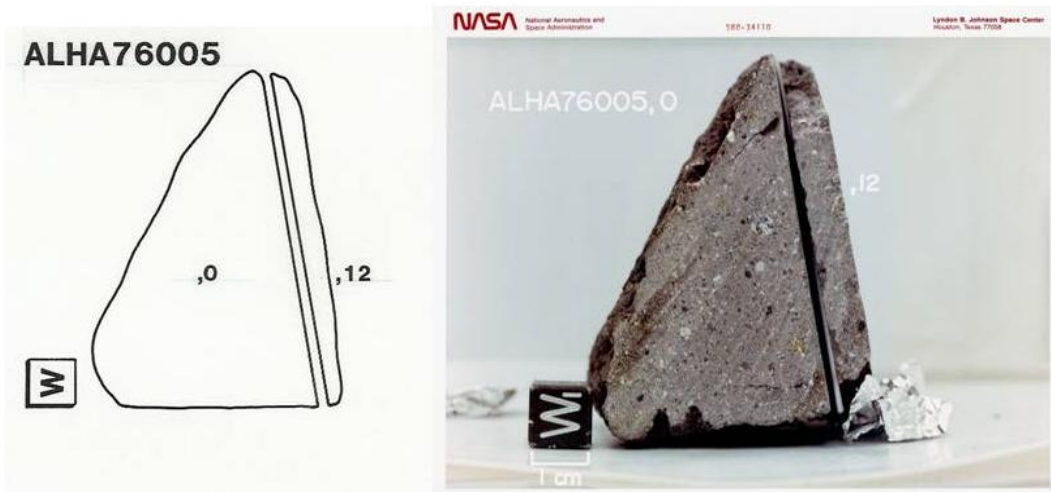


Figure 13: summary of HED oxygen isotopic measurements from Wiechert et al. (2004), with ALH 76005 and 78132 shown close to the center of the diagram.

**Petrogenesis:** Studies of the clasts within the separate masses of the pairing group indicate the possibility that many could have originated during the fractional crystallization of the same parent liquid(s) (Simon and Papike, 1981; Delaney et al., 1984). The textural diversity of the clasts, of course, suggests a range of thermal conditions and cooling histories for the intrusive and extrusive rock types found in the clasts within the pairing group.

**Pairing:** The pairing of the many samples in this group has been considered in most detail by Delaney et al. (1984) and is based on a combination of information – matrix composition, clast types, the absence of diagenitic material, and bulk composition.

**Processing: JSC**



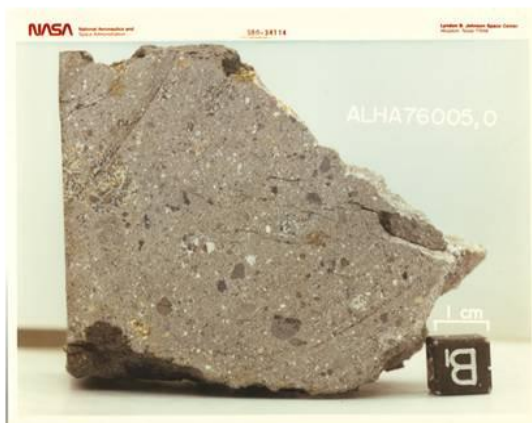
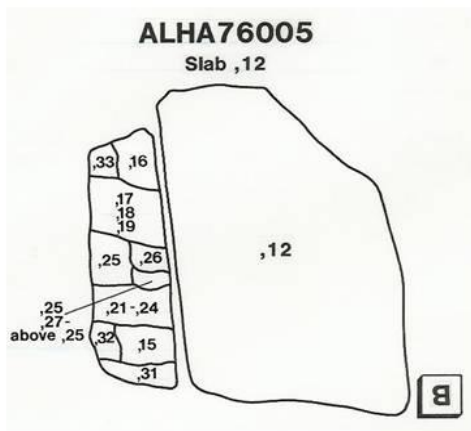
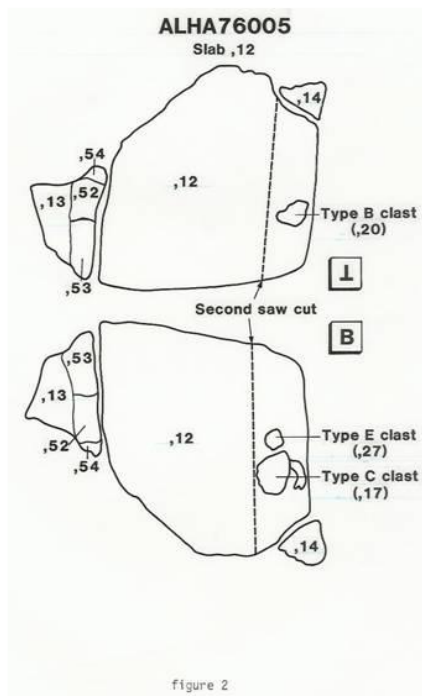


Figure 14: Processing photos and sketches (done by JSC MPL staff members) for the ALH 76005 eucrite. The slab (,12) was derived by bandsawing the main mass (,0). The slab was then subdivided according to the sketches and photos above.

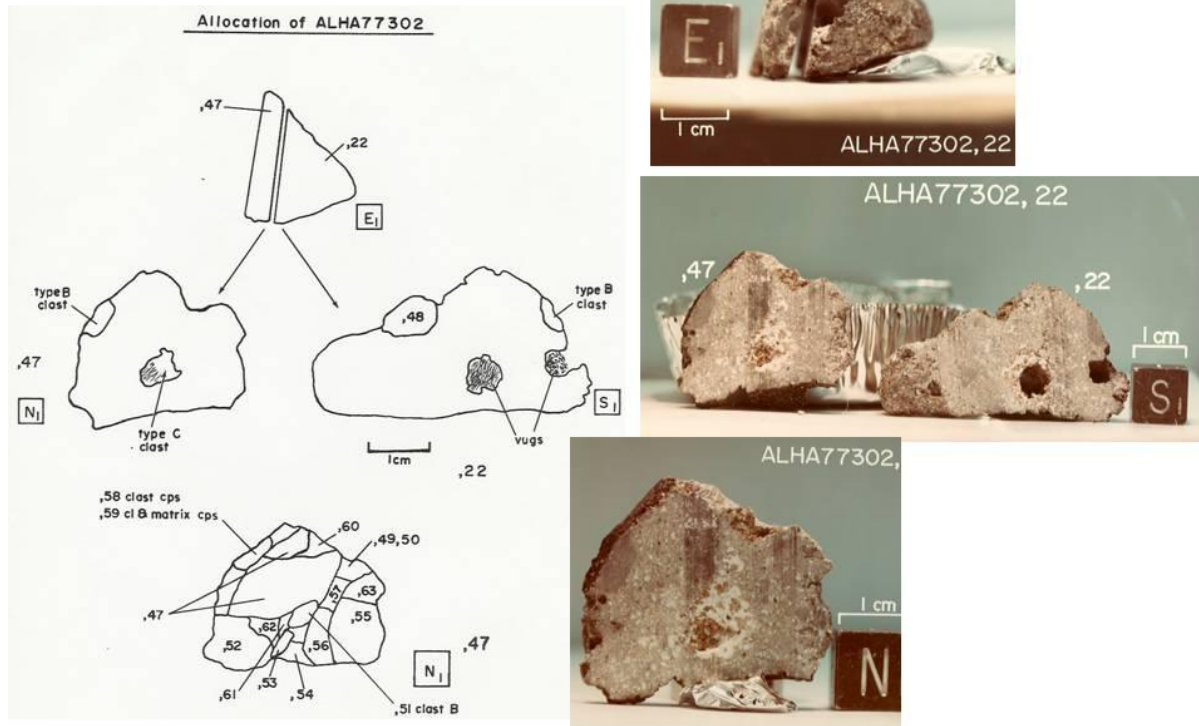


Figure 15: Processing photos and sketches (done by JSC MPL staff members) for the ALH 77302 eucrite. The slab (.47) was derived by bandsawing split .22. The slab was then subdivided according to the sketches and photos above.

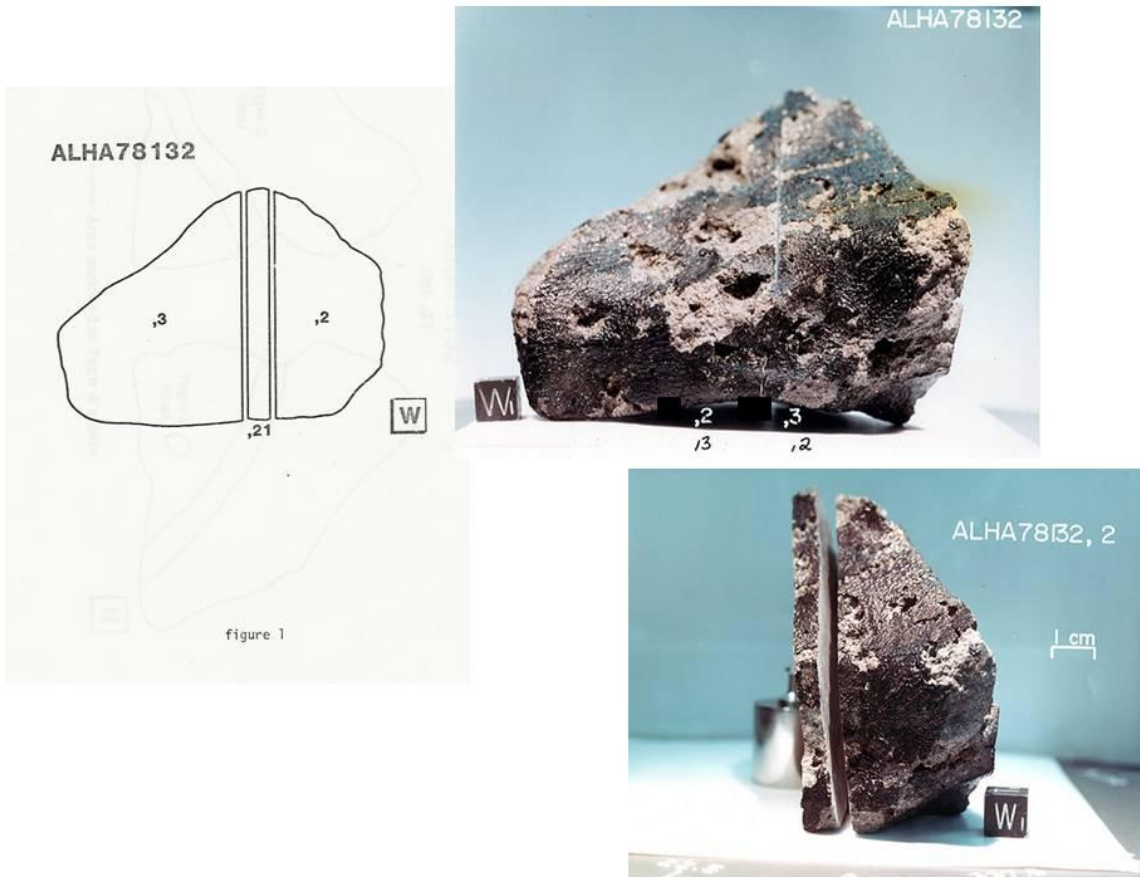


Figure 16: Processing photos and sketches (done by JSC MPL staff members) for the ALH 78132 eucrite. The slab (,21) was derived by bandsawing the main mass (,0); the geometry of the resulting halves - ,2 and ,3 – are shown. The slab ,21 as then subdivided according to the sketches and photos in Figure 17.

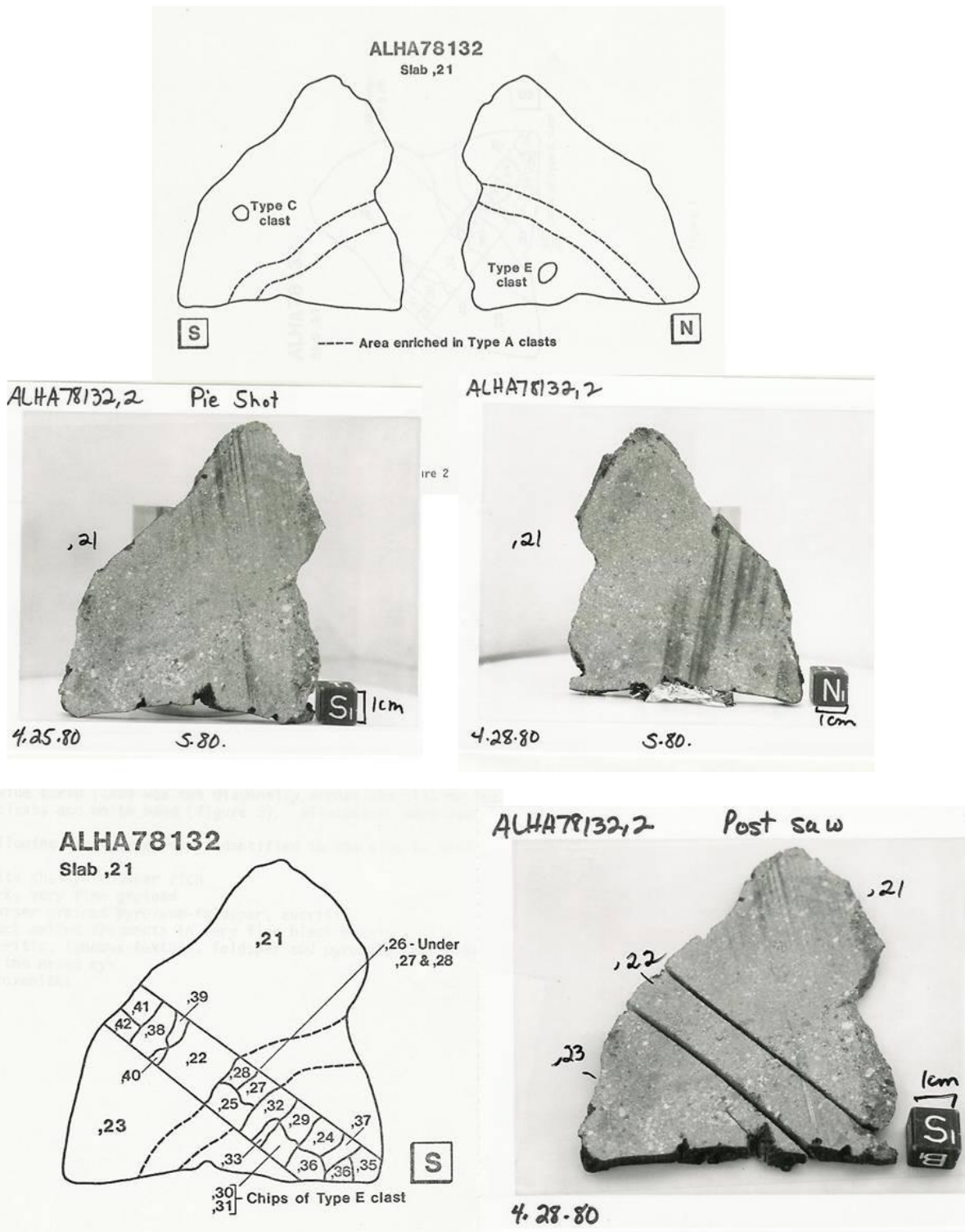


Figure 17: Processing photos and sketches (done by JSC MPL staff members) of the ALH 78132 slab (,21) and its subdivision.

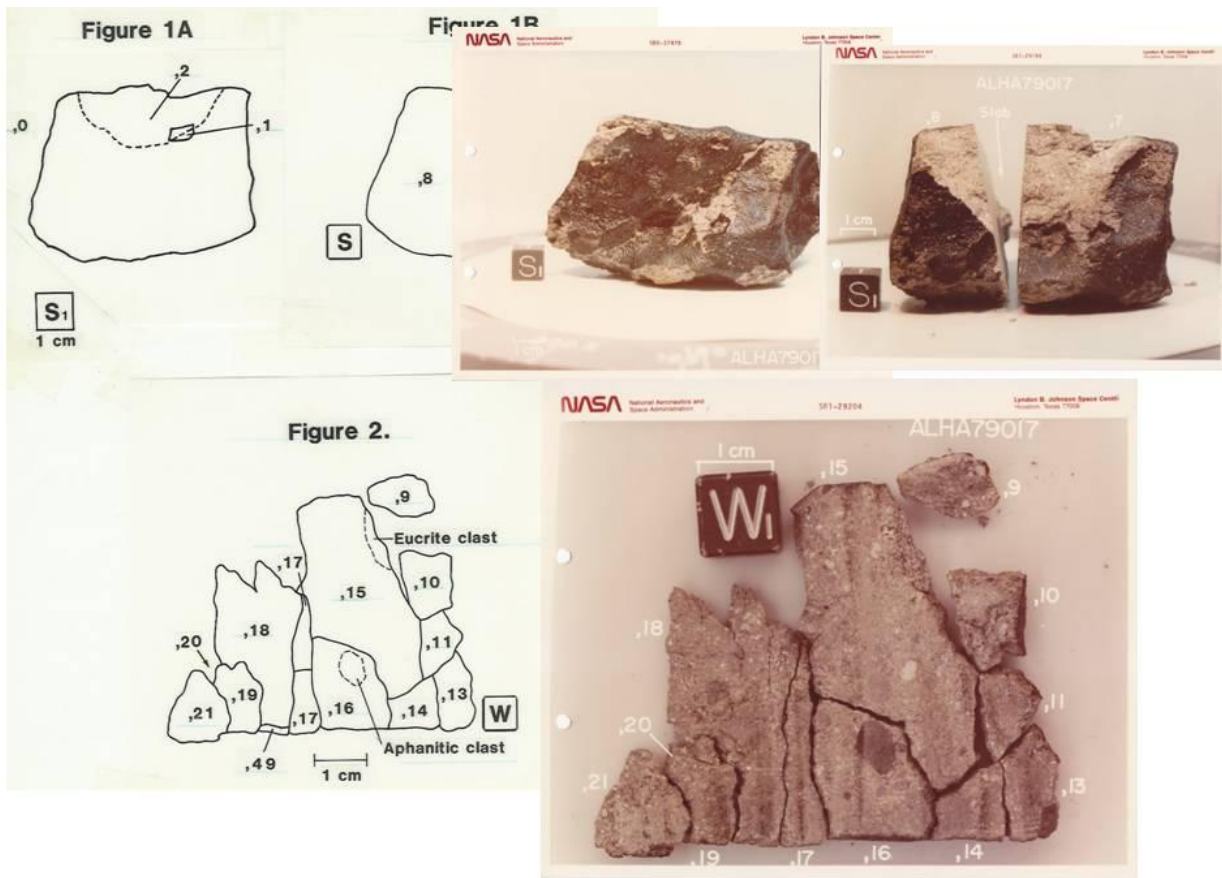


Figure 18: Processing photos and sketches (done by JSC MPL staff members) for the ALH 79017 eucrite. The slab was derived by bandsawing the main mass (,0). The slab was not coherent and broke into many pieces that were reconstructed and photographed as above. Two large pieces - ,15 and 16 - were subdivided further as summarized in Figure 19.

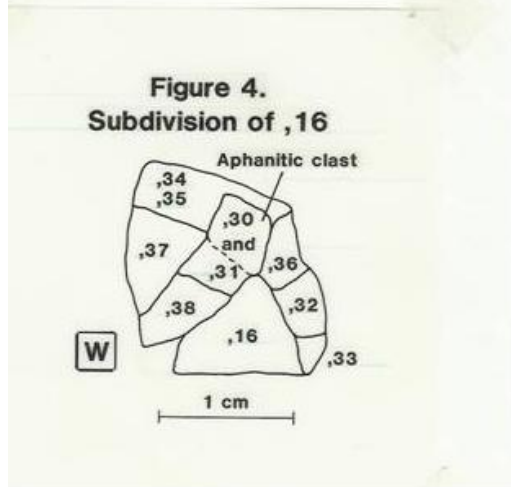
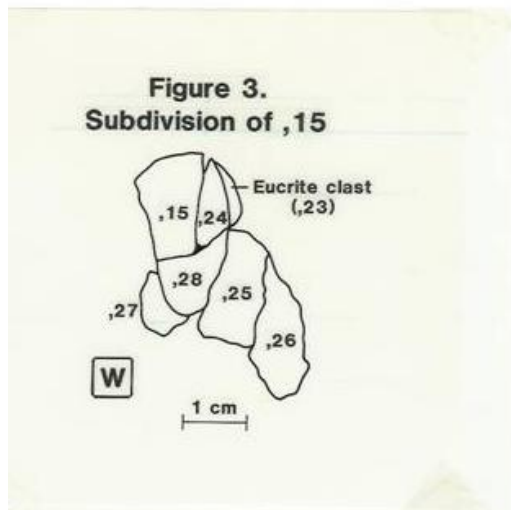


Figure 19: Processing photos and sketches (done by JSC MPL staff members) for subdivision of slab pieces of the ALH 79017 eucrite.

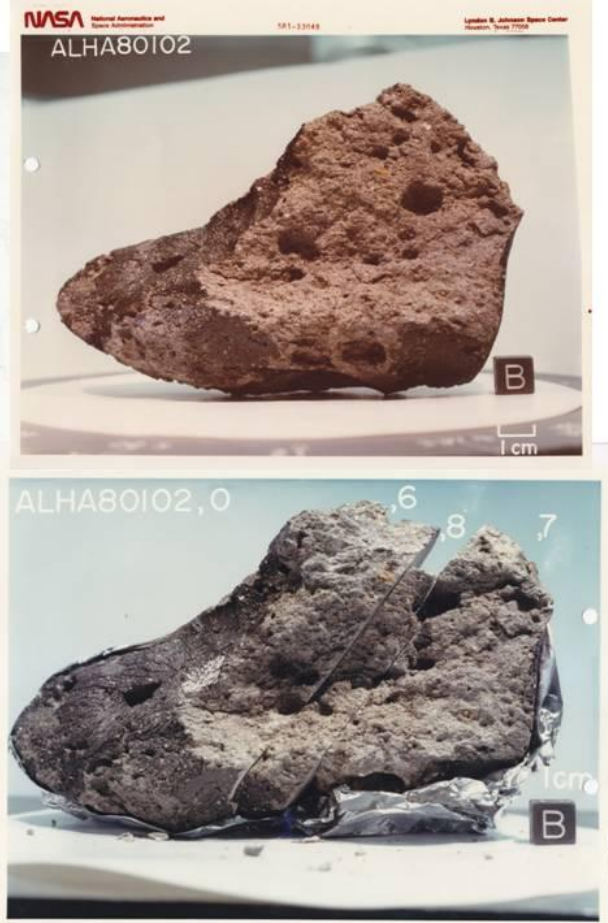
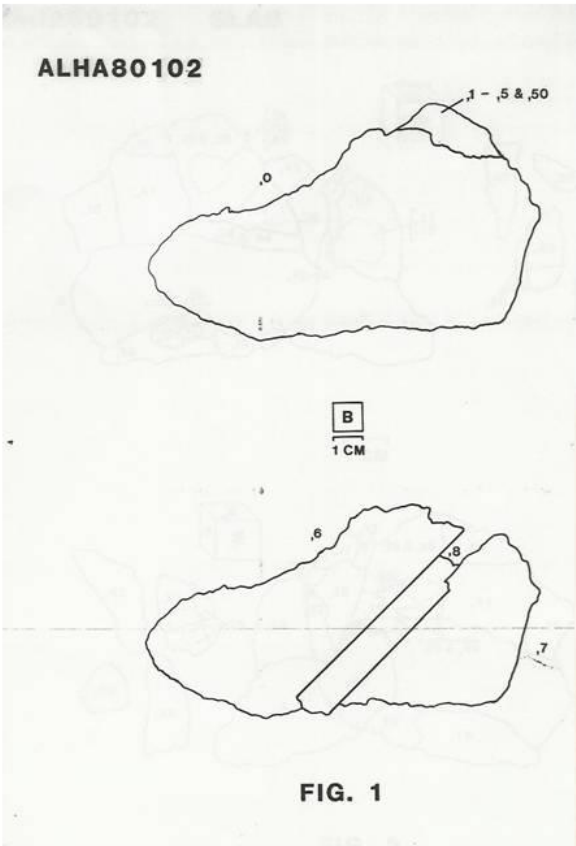


Figure 20: Processing photos and sketches (done by JSC MPL staff members) for the ALH 80102 eucrite. The slab (,8) was derived by bandsawing the main mass (,0). The slab was then subdivided according to the sketches and photos in Figure 21.

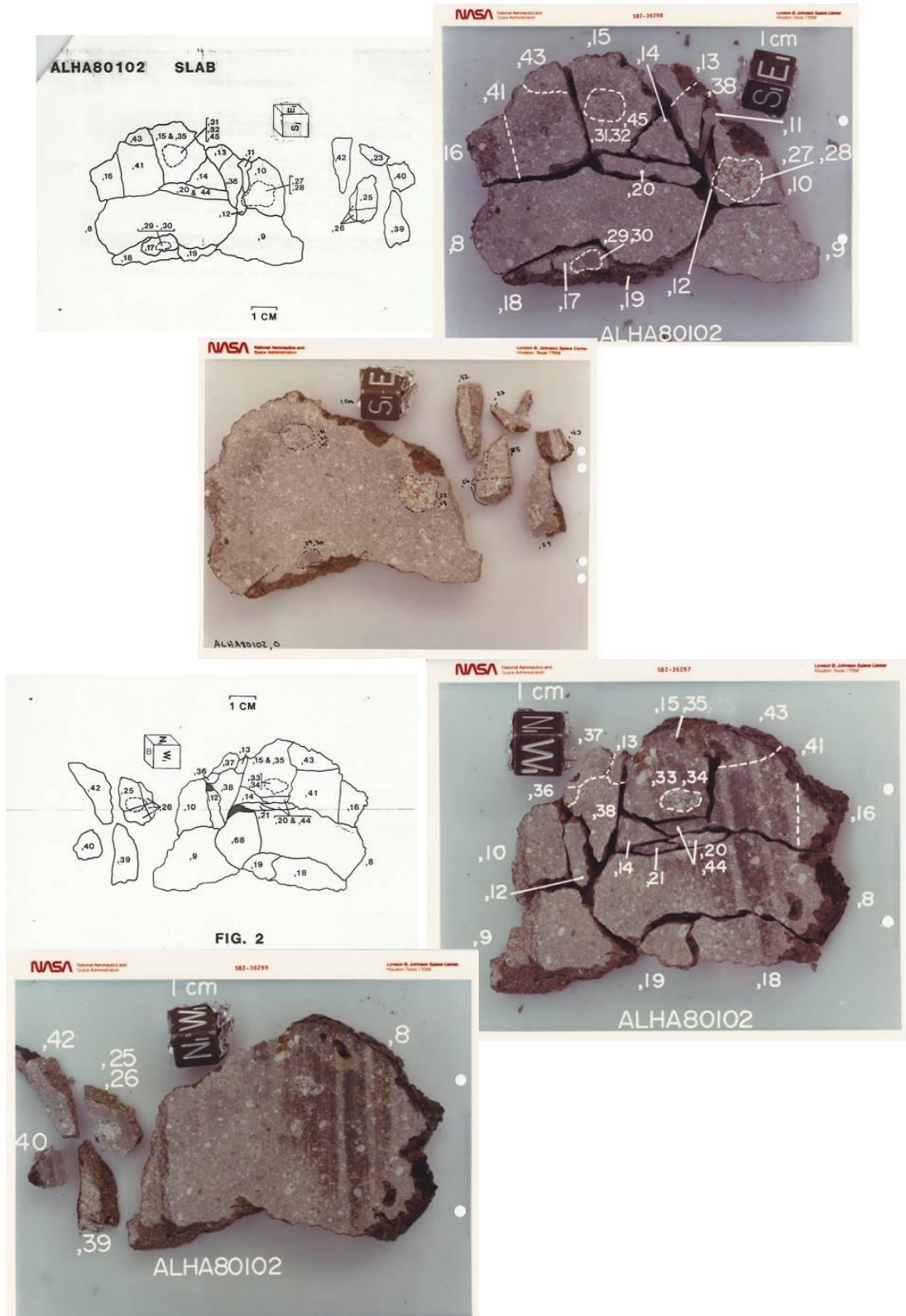


Figure 21: Processing photos and sketches (done by JSC MPL staff members) for subdivision of the slab (,8) of the ALH 80102 eucrite. The slab subdivision is shown from the two different sides.

**NIPR**

Several of the ALH 76005 pairing group samples were collected jointly with the National Institute for Polar Research (NIPR) in Tokyo, Japan. These samples are: ALH 76005, 77302, 78040, 78132, 78158, and 78165. These samples were split with the NIPR, and curated separately. Below are macroscopic and microscopic photos of the NIPR masses.

*Figure 22: NIPR photos of ALH 76005 (or ALH-765)*

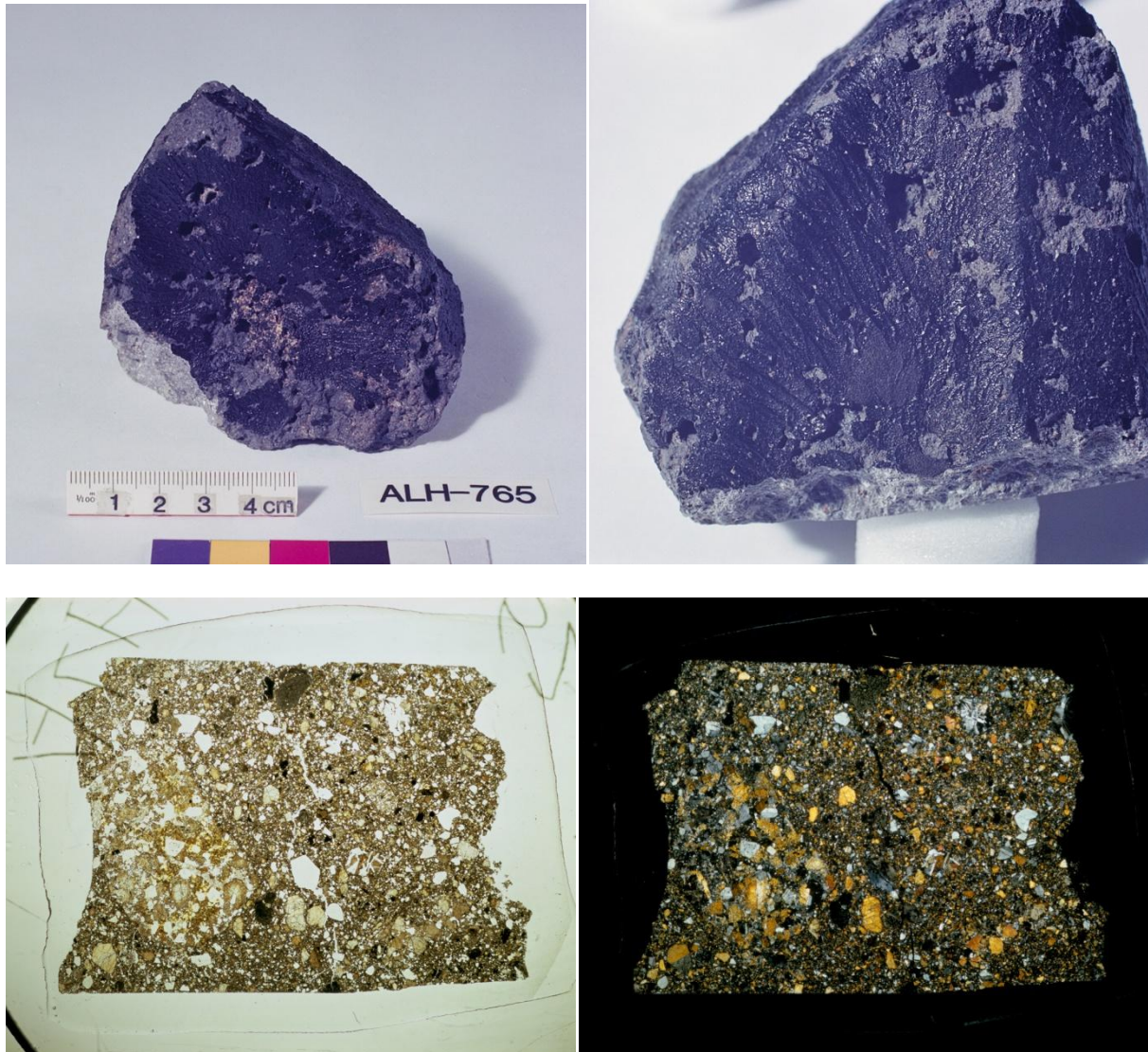


Figure 23: NIPR photos of ALH 77302



Figure 24: NIPR photos of ALH 78040



Figure 25: NIPR photos of ALH 78132



Figure 26: NIPR photos of ALH 78158

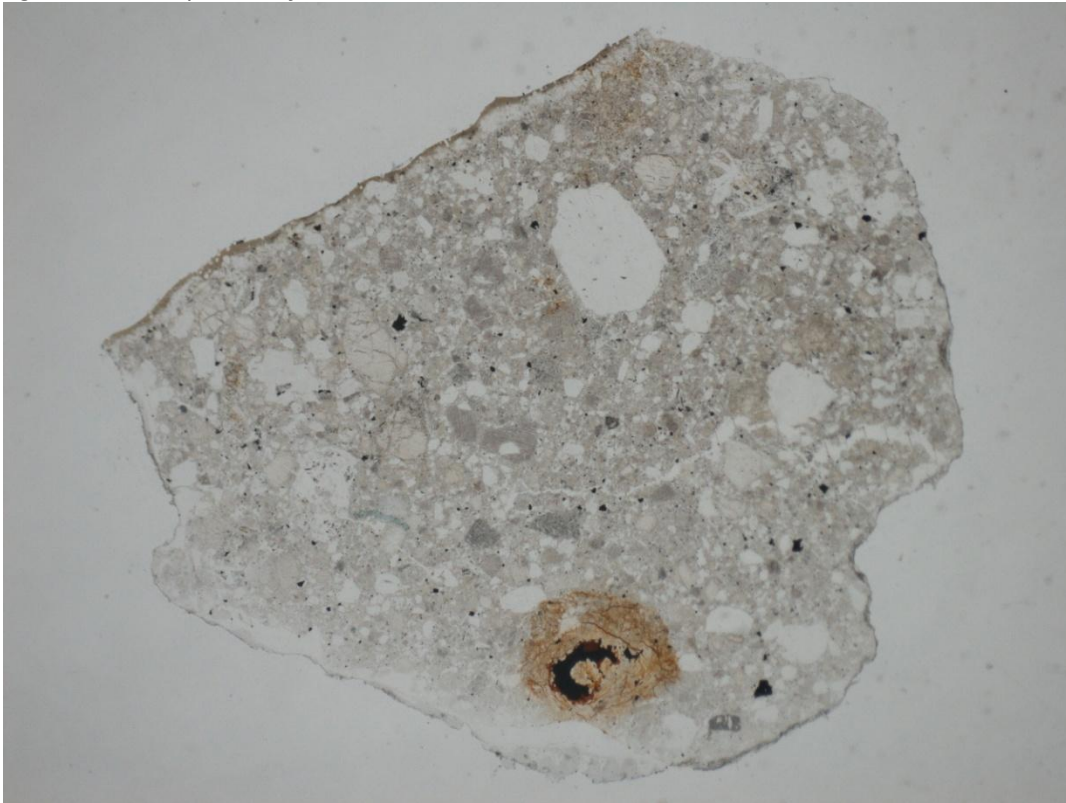


Figure 27: NIPR photos of ALH 78165

